Radially Softening Diffusive Motions in a Globular Protein

Serge Dellerue,* Andrei-J. Petrescu,† Jeremy C. Smith,‡ and Marie-Claire Bellissent-Funel*
*Laboratoire Léon Brillouin, CEA-Centre National de la Recherche Scientifique, CEA-Saclay, 91191 Gif-sur-Yvette, France, †Institute of Biochemistry, Splaiul Independentei 296, 77700 Bucharest, Romania, and ‡Lehrstuhl für Biocomputing, Interdisziplinäres Zentrum für Wissenschaftliches Rechnen, Universität Heidelberg, D-69120 Heidelberg, Germany

ABSTRACT Molecular dynamics simulation, quasielastic neutron scattering and analytical theory are combined to characterize diffusive motions in a hydrated protein, C-phycocyanin. The simulation-derived scattering function is in approximate agreement with experiment and is decomposed to determine the essential contributions. It is found that the geometry of the atomic motions can be modeled as diffusion in spheres with a distribution of radii. The time dependence of the dynamics follows stretched exponential behavior, reflecting a distribution of relaxation times. The average side chain and backbone dynamics are quantified and compared. The dynamical parameters are shown to present a smooth variation with distance from the core of the protein. Moving outward from the center of the protein there is a progressive increase of the mean sphere size, accompanied by a narrowing and shifting to shorter times of the relaxation time distribution. This smooth, "radially softening" dynamics may have important consequences for protein function. It also raises the possibility that the dynamical or "glass" transition with temperature observed experimentally in proteins might be depth dependent, involving, as the temperature decreases, progressive freezing out of the anharmonic dynamics with increasing distance from the center of the protein.

INTRODUCTION

Both experiment and simulation have demonstrated the wide range of motions in proteins, some of which are required for function (Reat et al., 2000; Heikal et al., 2000; Ma et al., 2000; Balabin and Onuchic, 2000; Vitkup et al., 2000; Brooks et al., 1988; McCammon and Harvey, 1987). At physiological temperatures, internal motions in proteins are partly vibrational and partly diffusive (Hinsen et al., 2000; Amadei et al., 1999; Hayward et al., 1995; Kneller and Smith, 1994; Cusack et al., 1988; Elber and Karplus, 1987). The diffusive motion is of particular interest in the context of the dynamical or "glass" transition, which is observed experimentally at ~180–220 K. Above this transition, the diffusive motions are activated, whereas below it only vibrations exist. In some cases (although not all (Daniel et al., 1998)) the activation of the diffusive motions has been correlated with the onset of protein activity (Ferrand et al., 1993; Rasmussen et al., 1992; Frauenfelder et al., 1991; Parak et al., 1980).

The characterization of internal diffusion in proteins is complicated by the variety of the motions present. These involve groups of atoms undergoing a plethora of continuous or jump-like diffusive dynamics (Zanotti et al., 1997, 1999; Receveur et al., 1997; Yamasaki et al., 1995; Kneller and Smith, 1994; Daragan and Mayo, 1993; Elber and Karplus, 1987). It is thus clearly of interest to see whether it is possible to capture the essence of this complexity by describing it with only a small set of phenomenological variables. This provides a challenge with important consequences both for interpreting experimental results and for simplifying, in a meaningful way, the data generated from molecular dynamics (MD) simulation. Here we attack this problem by analyzing dynamic neutron scattering experiments using MD and analytical modeling.

Dynamic neutron scattering is the most direct probe of diffusive protein dynamics on the 10^{-12}–10^{-9}s timescale (Smith, 1991). In recent years dynamic neutron scattering experiments on proteins have solicited increasing interest (e.g., Zaccai, 2000a,b; Reat et al., 1998, 2000; Dunn et al., 2000; Bu et al., 2000; Zanotti et al., 1997, 1999; Perez et al., 1999; Cordone et al., 1999; Daniel et al., 1999; 1998, Fitter et al., 1998; Diehl et al., 1997; Bellissent-Funel et al., 1997; Receveur et al., 1997). The measured quantity is the dynamic structure factor, S, which is a function of the scattering wave vector, q and the energy transfer, ω. In proteins, $S(q, \omega)$ is dominated by the incoherent component resulting from self-correlations in the hydrogen atom positions. Because these are evenly distributed throughout the protein, the experiment gives a global view of protein motions.

The geometry and time dependence of the diffusive motion are given by the elastic scattering and the quasielastic broadening of the elastic peak (Bee, 1988). However, the interpretation of neutron scattering data on proteins directly using analytical models of atomic dynamics is complicated by the existence of the wide repertoire of diffusive motions mentioned above. To overcome this problem, MD simulation can be used as a stepping stone between experiment and analytical theory (Smith, 1991, 1997, 2000). MD is complementary to neutron scattering because it probes motions on the same length and time scales and because the scattering can be directly computed from the simulated atomic trajectories without any significant approximation. Thus, the MD trajectory can be decomposed to identify relevant

Received for publication 13 March 2001 and in final form 25 May 2001.
Address reprint requests to Jeremy C. Smith, Lehrstuhl für Biocomputing, IWR, Universität Heidelberg, Im Neuenheimer Feld 368, D-69120 Heidelberg, Germany. Tel.: +49-6221-548857; Fax: +49-6221-548868; E-mail: biocomputing@iwr.uni-heidelberg.de.

0006-3495/01/09/1666/11 $2.00

motions that contribute to the measured scattering. In favorable cases, the dynamics can then be modeled using analytical techniques (Hinsen et al., 2000; Souaille et al., 1996a,b).

We use here this combined approach of neutron scattering, MD simulation and analytical modeling to obtain a description of protein dynamics that includes the diversity of amplitudes and relaxation times experienced by atoms in the protein. With this approach, it is possible to quantify and differentiate between the backbone and side-chain contributions to the neutron scattering spectrum both in terms of the amplitudes of the motions and the distributions of their associated dynamical relaxation times. It is also possible to show that the average dynamical properties vary smoothly with distance from the protein core, involving a gradual increase of the diffusive amplitudes and a narrowing and shift to shorter times of the distribution of relaxation processes. The possible implication of this for glass transition behavior and protein function is discussed.

METHODS

The neutron scattering experiments were performed on amorphous powders of C-phycocyanin hydrated to 0.52 g protein/g D_2O. To simulate the hydrated amorphous powder system, the MD calculations were performed using a model consisting of a single hydrated C-phycocyanin $\alpha\beta$ molecule together with its three chromophores and explicit water hydrating the protein to a similar level as in the experiment.

Quasielastic neutron scattering experiments

The sample used was 170 mg hydrated C-phycocyanin powder. To maximize the contribution from the protein motions under controlled conditions, the experiments were performed using fully-deuterated solvent and hydrogen-deuterium exchanged protein. The consequent partial deuteration of the protein is limited to the exchangeable hydrogens. Under these conditions the scattering is dominated by the unexchanged protein hydrogens.

The experiments were performed on the Mibemol spectrometer at the Orphée Reactor, LLB, (Saclay, France). The incident wavelength was 6 Å, the experimental resolution 96 μeV (full-width at half-maximum) and the q-range 0.46–1.95 $Å^{-1}$. The sample container was a flat aluminium cell of 1.5-mm thickness. The scattering of the empty cell was subtracted from that of the sample. The differences in detector sensitivity were corrected using the scattering of vanadium. To improve statistics, the detectors were grouped in sets of ten. Due to the high transmission of the samples (95–97%) the spectra did not need to be corrected for multiple scattering.

Molecular dynamics simulation

The program used for the MD simulation was CHARMM with force field and version 22 (Brooks et al., 1983; MacKerell et al., 1998). The water was modeled using the TIP3P potential (Jorgensen et al., 1983). To hydrate the protein, a box of water with the standard liquid water density and 90 × 60 × 45-Å dimensions was equilibrated with CHARMM. The water molecules with oxygen atoms within 2.6 Å or further than 4.7 Å from any protein heavy atom were deleted. 5 nonstructural water molecules, found in interior pockets but not found crystallographically, were also eliminated. Using this procedure about one-and-a-half water layers remained, corresponding to a hydration of 0.6 g/g. The final model contained 1100 water molecules forming a system of 8417 atoms.

The simulation was performed in the microcanonical (NVE) ensemble. The non-bonded cutoff distance was 14 Å. Smoothing of the nonbonded interactions was performed with the switch method applied from 9 to 13 Å (Brooks et al. 1983). Bonds containing hydrogens were constrained with SHAKE (Ryckaert et al., 1977), allowing a 2-fs timestep. The system was subjected to 5000 steps of adopted-basis Newton–Raphson minimization, heated in 5 K increments for 10 ps and equilibrated for 100 ps. The production dynamics was for 1 ns, long enough to adequately sample the motions detected by the neutron instrument. The RMS deviation of the backbone atoms from the x-ray crystal structure was 1.4 Å at the end of the simulation, indicating that the protein had preserved its three-dimensional structure.

Theoretical analysis

Calculation of neutron scattering properties from MD simulation

Molecular dynamics simulation provides the position of each atom i as a function of time, $r_i(t)$. To compute the dynamic structure factor, $S(q, \omega)$, the appropriate time correlation function must be calculated. This is the incoherent intermediate scattering function, $I_{inc}(q, t)$ given by

$$I_{inc}(q, t) = \sum_i b_{i,inc}^2 \langle e^{i\mathbf{q}\cdot(\mathbf{r}_i(t)-\mathbf{r}_i(0))}\rangle, \quad (1)$$

where $b_{i\ inc}$ is the incoherent scattering length.

Because the thermal and orientation averages required for isotropic powder scattering are uncorrelated, the following equation can be derived:

$$I_{inc}(q, t) = \sum_i b_{i,inc}^2 \left\langle \frac{\sin(|\mathbf{q}| \cdot |\mathbf{r}_i(\tau + t) - \mathbf{r}_i(\tau)|)}{|\mathbf{q}| \cdot |\mathbf{r}_i(\tau + t) - \mathbf{r}_i(\tau)|} \right\rangle. \quad (2)$$

This function was normalized such that $I(q, 0) = 1$. The contribution to the scattering from sub-systems of atoms can be calculated by simply restricting the summation in Eq. 2.

For comparison with experiment $I_{inc}(q, t)$ was convoluted with the experimental instrumental resolution function, $I_{res}(q, t)$ then numerically Fourier transformed. This yields the dynamic structure factor,

$$S(q, \omega) = \frac{1}{\pi} \int_0^\infty I_{inc}(q, t) I_{res}(q, t) \cos \omega t \, dt. \quad (3)$$

To understand the origin of the quasielastic scattering, the intermediate scattering function, $I_{inc}(q, t)$ computed from the MD trajectory was fitted with the following commonly-used form (Bée, 1988):

$$I_{inc}(q, t) = (1 - A(q))\phi(q, t) + A(q). \quad (4)$$

Here $A(q)$ and $(1 - A(q))\phi(q, t)$ are the elastic and quasielastic components of $I_{inc}(q, t)$, respectively. $A(q)$ is the elastic incoherent structure factor. The time dependence of the quasielastic component is given by $\phi(q, t)$. It was found to be impossible to fit the simulation-derived $I_{inc}(q, t)$ with a single exponential time dependence. Therefore, $\phi(q, t)$ is modeled here with a Kohlrausch–William–Watts stretched exponential,

$$\phi(q, t) = \exp\{-[t/\tau(q)]^{\beta(q)}\}. \quad (5)$$

Stretched exponentials are commonly used to describe relaxation processes in strongly interacting disordered systems. The exponentials describe a distribution of relaxation times, reflecting the diversity of dynamical timescales in the system. The function in Eq. 2 was introduced in the nineteenth century by Kohlrausch to describe the relaxation of electrical polarization in glassy materials. Later, Williams and Watts used this function to fit the

α-relaxation of the electrical variables in glassy dynamics (Williams and Watts, 1970). Since then, the Kohlrausch–William–Watts function is almost omnipresent in the description of stretched relaxation, being preferred to other empirical functions due to its usefulness in the theory of asymmetric probability distributions. A large number of physical systems have been shown to present Kohlrausch–Williams–Watts relaxation behavior, and, consequently, a number of theories have been proposed to explain it (Götze and Sjögren, 1992 and Kurzinsky, 1998). For example, stretched exponential behavior describes systems for which the spectrum of relaxation times presents the so-called self-similarity symmetry or time scaling property. Glassy materials may be examples of such systems. Stretched exponential behavior also arises in the mode coupling theory of glass transitions (Götze and Sjögren, 1992). In mode coupling theory, the slowing-down of structural relaxation with decreasing temperature is described microscopically as being due to hindering of individual particle dynamics by neighbours. The Kohlrausch–William–Watts function has also been used in the interpretation of quasielastic neutron scattering on supercooled water (Sciortino et al. 1996).

Spin-glass models have also been invoked to describe protein energy landscapes (e.g., Goldstein et al., 1992; Stein, 1985). To explain time scaling, fractal time or fractal space have been invoked. The former results from a hierarchy of barrier heights in the potential energy landscape (Schlesinger, 1988; Frauenfelder et al. 1988) whereas the latter corresponds to a hierarchy of bottlenecks (entropy barriers) in the passages between conformations on the free energy surface (Blumen and Schnorer, 1990).

Analysis of A(q)

The simulation-derived scattering functions were interpreted with an analytical model in which the atoms diffuse confined in a spherical volume. For spheres of a given radius a, $A(q)$ is given by

$$A(q) = \left[\frac{3j_1(qa)}{qa}\right]^2$$

with (6)

$$j_1(qa) = \frac{\sin(qa) - (qa)\cos(qa)}{(qa)^2},$$

where $j_1(qa)$ is the first-order spherical Bessel function (Volino and Dianoux, 1980).

Here, to account for the diversity of amplitudes experienced by atoms in a protein we choose to use a distribution of sphere radii rather than one single radius. The probability distribution of the atoms as a function of a discrete set of radii, $\{a_i\}$ is denoted $p(a_i)$. The elastic component $A(q)$ then reads

$$A(q) = \frac{1}{\sum_i p(a_i)\Delta a_i} \sum_i p(a_i) f_i(q),$$

where:

$$p(a_i) = \begin{cases} p_i & \alpha \in \left\{a_i - \dfrac{\Delta a_i}{2}, \quad a_i + \dfrac{\Delta a_i}{2}\right\} \\ 0 & \alpha \notin \left\{a_i - \dfrac{\Delta a_i}{2}, \quad a_i + \dfrac{\Delta a_i}{2}\right\} \end{cases}$$

and (7)

$$f_i(q) = \int_{a_i - \Delta a_i/2}^{a_i + \Delta a_i/2} A(q\alpha)\, d\alpha = \int_{a_1 - \Delta a_i/2}^{a_i + \Delta a_i/2} \left[\frac{3j_1(q\alpha)}{q\alpha}\right]^2 d\alpha.$$

Fitting to $A(q)$ involved a nonlinear least squares procedure to optimize $p(a_i)$. $p(a_i)$ was found to be independent of the discretization step used for $\{a_i\}$.

RESULTS

In a first step of the analysis the dynamic structure factor was computed from the MD trajectory and compared with experiment. In Fig. 1 are presented the dynamic structure factor, $S(q, \omega)$ obtained experimentally and from the simulation. In both cases, the quasielastic intensity, which appears as a broadening of the elastic peak, increases with q. The experiment and simulation agree for most of the q range, although for the very highest q the quasielastic component (the broadening under the elastic peak) is slightly wider in the simulation, indicating that the dynamics in the simulation may be somewhat faster than in the experiment.

The fits of Eq. 4 are shown in Fig. 2 for the backbone and side chains. Clearly, for both the side chains and the backbone Eq. 4 fits the data well. This indicates that stretched-exponential behavior is appropriate for describing the time-dependence of internal protein motions. The results of the fitting are the relaxation time $\tau(q)$ and the stretch parameter, $\beta(q)$. These are presented in Figs. 3, *A* and *B*. As can be seen, there are marked differences between the behavior of the backbone and side chains. For both, the stretch factor $\beta(q)$ reaches a constant value for $q > 2$ Å, of $\beta \sim 0.40$ for the main chain and $\beta \sim 0.27$ for the side chains (see Fig. 3b). The further the exponent β is from 1.00 the greater the nonexponentiality in the time-dependence of the relaxation behavior. Therefore, although both subsystems exhibit highly nonexponential dynamics, this is more marked for the side chains indicating a wider distribution of relaxation processes.

In Fig. 3 *A*, the initial low q plateau of $\tau(q)$ is followed by power law behavior. Linear fitting results, presented in the inset to Fig. 3a, yield $\tau^\beta \sim q^{-1.39}$ for the backbone and $\tau^\beta \sim q^{-1.43}$ for the side chains for $q > 3.5$ Å^{-1} and $q > 2.2$ Å^{-1}, respectively. This information can be used to compare the internal motions in the protein with two extreme cases—the heterogeneous and homogenous dynamical scenarios. In the heterogenous case, the stretched exponential results from a superposition of single exponentials from atoms with different relaxation times. It can be shown that this gives $\tau(q) \sim q^{-2}$ (Arbe et al. 1998). In the homogenous case, all the relaxation processes are identical but nonexponential—each is then characterized by the same stretched exponential. In this case, $\tau \sim q^{-2/\beta}$. For $q > \sim 2$ Å^{-1} in Fig. 3 *B* (where β is constant), the value of $-2/\beta$ is -5.0 for the backbone and -7.4 for the side chains. In comparison, the corresponding values obtained from the fits in Fig. 3 *A* are -3.4 for the backbone and -5.3 for the side chains. Therefore both the side chains and backbone show behavior intermediate

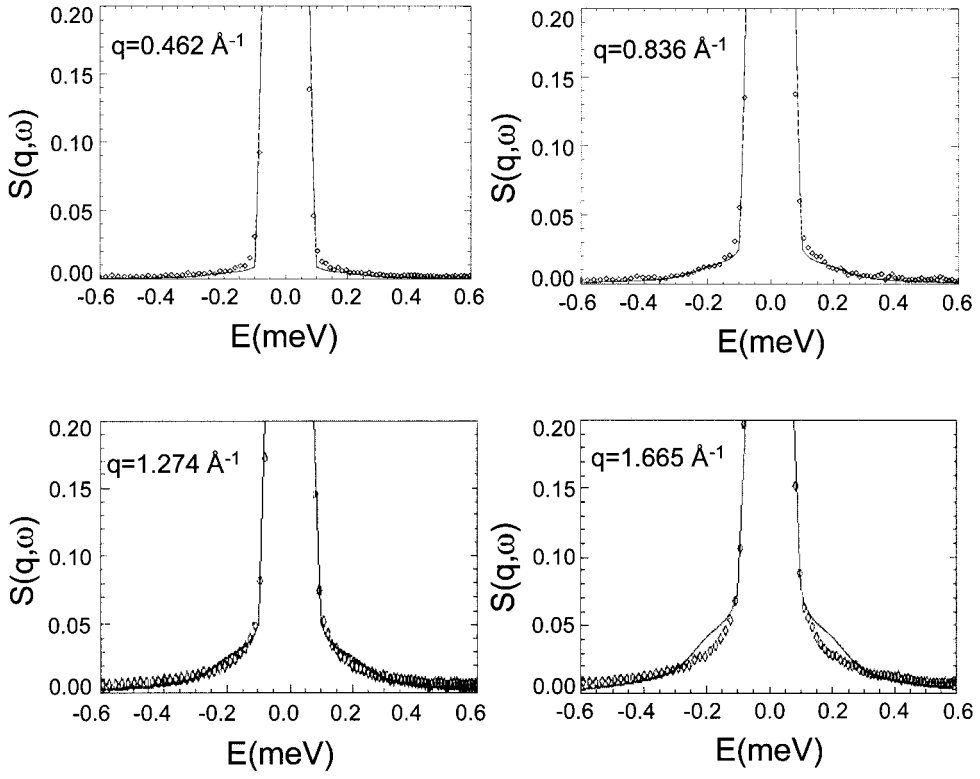

FIGURE 1 Experimental and simulation-derived $S(q, \omega)$ for C-phycocyanin hydrated with D_2O.

between homogeneous ($-2/\beta$) and heterogeneous (-2.0), with the side chains, however, somewhat closer to homogeneous dynamics.

The simulation-derived scattering functions were interpreted with an analytical model derived by extending a simple description of confined diffusion. In this model, the atoms diffuse in a spherical volume. The analytical expressions for the scattering functions derived for the case of a uniform sphere radius (see Methods) have been widely used in the interpretation of quasielastic neutron scattering experiments. The determination that the side-chain motion in globular proteins contains a strong liquid-like nonvibrational confined diffusive component at physiological temperatures is consistent with the use of this model for proteins (Kneller and Smith, 1994). In combination with neutron scattering, the model in this

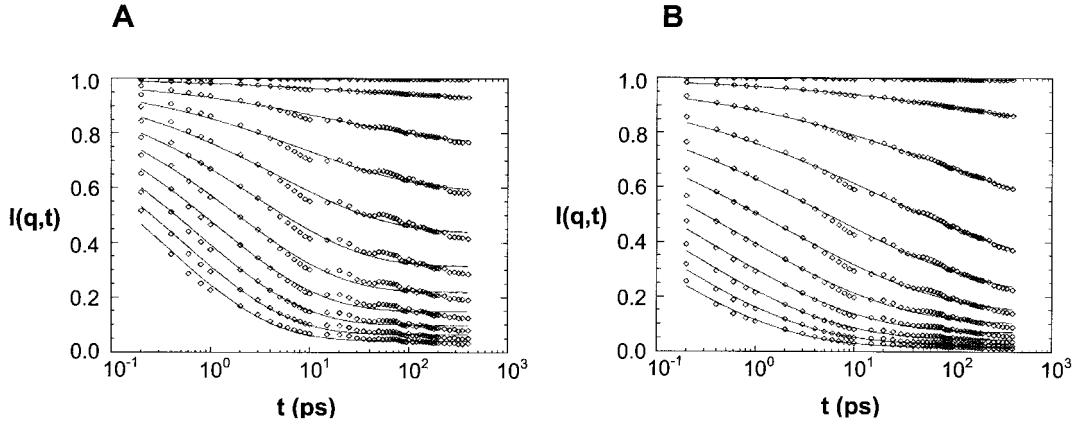

FIGURE 2 Simulation-derived intermediate scattering function together with fitted stretched exponential function. (*A*) Backbone atoms. (*B*) Side-chain atoms. The oscillations at large t in the simulation data arise from long time statistical errors. *Diamonds*, $I(Q, t)$ calculated from the trajectories of the MD simulations. The full line gives the result of the fit using Eq. 4. From the top to the bottom, the values of Q are: 0.1, 0.5, 1.2, 2.5, 3, 3.5, 4, 4.5, and 5 $Å^{-1}$. $T = 292$ K.

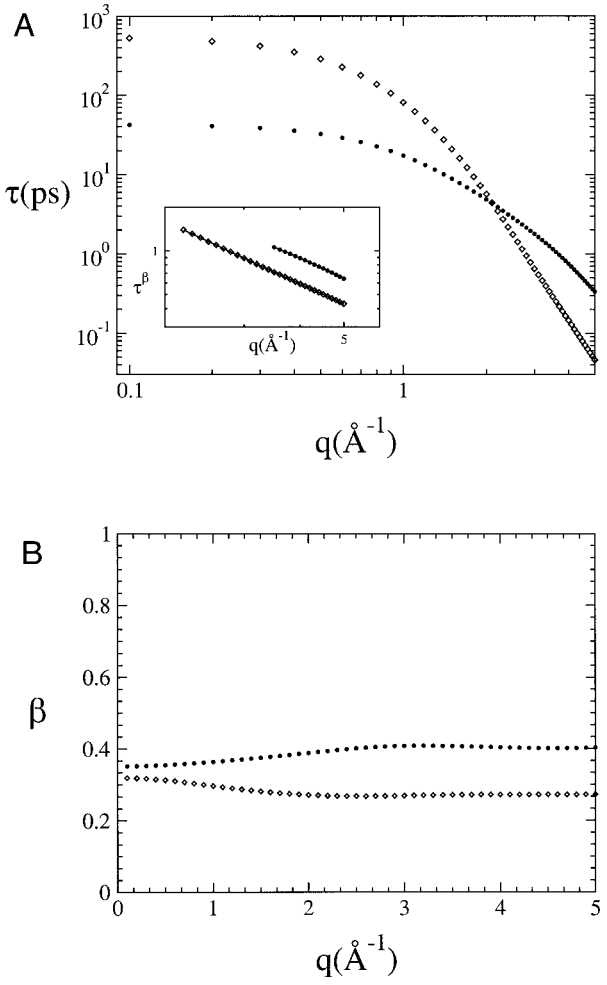

FIGURE 3 Dynamical parameters for the backbone (*filled circles*) and side chains (*open diamonds*). (*A*)τ versus q. (*B*) β versus q.

simple form has been used to describe water dynamics at the surface of hydrated powders of C-phycocyanin (Belissent-Funel et al., 1992) motions in parvalbumin (Zanotti et al., 1997, 1999) and the dynamical changes in phosphoglycerate kinase upon unfolding (Receveur et al., 1997).

The q dependence of $1/\tau(q)$ is shown in Fig. 4 *B* for the ideal cases of free unconfined diffusion and diffusion in a sphere. For unconfined diffusion, $1/\tau(q)$ follows a Dq^2 "law" where D is the diffusion coefficient, whereas, for diffusion confined to a sphere, $1/\tau(q)$ is independent of q for $q < \pi/R$ and then for $q > \pi/R$ also varies as Dq^2 (Volino and Dianoux, 1980). Comparison of Fig. 4 *B* with the equivalent simulation results in Fig. 4 *A* confirms that the hydrogen atoms in the protein indeed undergo confined diffusion. The simulation-derived $\tau(q)$ profile is consistent with a description of diffusion in spheres with a distribution of radii—this leads to a more gradual gradient change than for the single-sphere case in which the plateau ends promptly at $q = \pi/R$. Also visible in Fig. 4 is the marked difference between the side chain and backbone dynamics. The diffusive regime (linear in q^2) is reached for the side chains at $q^2 > \sim 2$ Å^{-2}, whereas, for the backbone only for much higher q^2, $> \sim 10$ Å^{-2}. This indicates that the average volume in which the backbone atoms are confined is smaller than for the side chains.

The elastic incoherent structure factor, $A(q)$ is determined by the geometry of the space accessed by the atoms of the system (Bée, 1988). $A(q)$ is presented in Fig. 5 *A*. Here, given the above considerations and to account for the diversity of amplitudes experienced by atoms in a protein, $A(q)$ was fitted with a model incorporating a

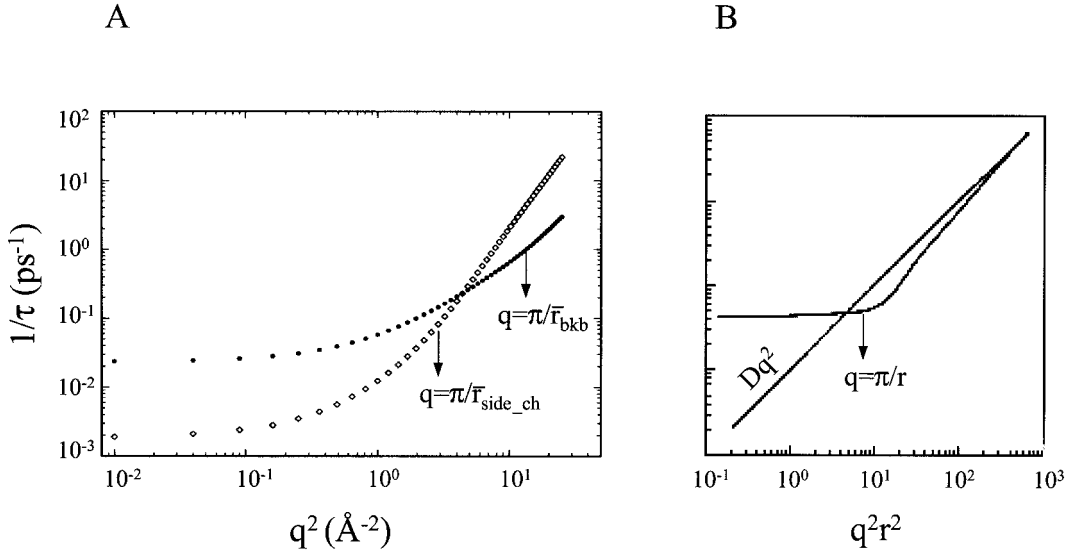

FIGURE 4 $1/\tau$ versus q^2. (*A*) Backbone (*filled circles*) and side chains (*open diamonds*) of the protein. (*B*) Ideal cases: free-diffusion (Dq^2 law) and diffusion in a sphere.

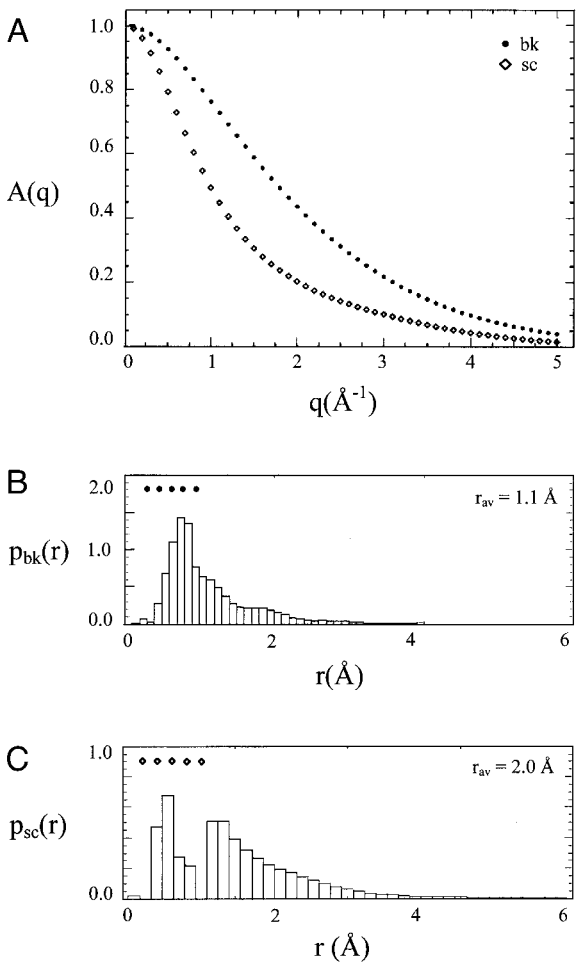

FIGURE 5 Geometry of the diffusive motions. (*A*) The elastic incoherent structure factor $A(q)$ for the backbone (bk) and side chains (sc). (*B*) The fitted distribution of sphere radii for the backbone. (*C*) The fitted distribution of sphere radii for the side chains.

distribution of sphere radii rather than one single radius (see Methods, Eq. 7). The distributions obtained are shown in Fig. 5, *B* and *C*, for the backbone and side chains, respectively. The geometries sampled in the confined diffusion of the side chains and the backbone significantly differ. For the backbone, a single population results, centered on ~1 Å, whereas, for the side chains, two populations are seen, one at ~1 Å and a wider distribution with a peak at ~1.7 Å. In Fig. 6 is shown the time dependence of the mean-square displacement for the side chain and backbone atoms. The long-time values are ~1.5 Å^2 for the backbone and ~3.5 Å^2 for the side chains, in close agreement with the corresponding fitted mean sphere radii. The smaller average sphere radius for the backbone than for the side chains is also in agreement with the difference in the relaxation behavior shown in Fig. 4 *A*, in which the diffusive regime for the backbone is reached at higher q^2 than for the side chains. The q^2 value corresponding to the reciprocal mean sphere radius is indicated on Fig. 4 *A* and indeed coincides with the onset of the linear diffusive regime, in harmony with the diffusion-in-a-sphere theory (Volino and Dianoux, 1980). Further analysis showed no clear link between the distance from the backbone and the amplitude of the confined side-chain diffusion as estimated from the mean sphere radius. For example, the distributions for the C_γ valine methyl groups and the C_δ and C_γ isoleucine groups are all centered at ~1 Å, whereas those of C_δ of leucine and C_γ of threonine are peaked at ~1.6 and ~1.4 Å, respectively.

We now examine the radial dependence of the dynamical parameters, i.e., how they vary with distance from the center of mass of the protein. To examine this, the protein was partitioned into eight concentric shells, as

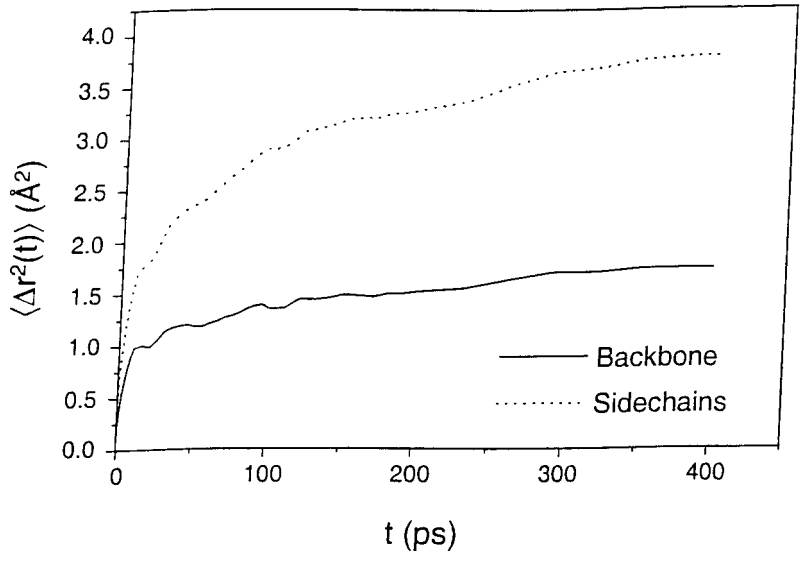

FIGURE 6 Time dependence of mean-square displacement for backbone and side-chain atoms.

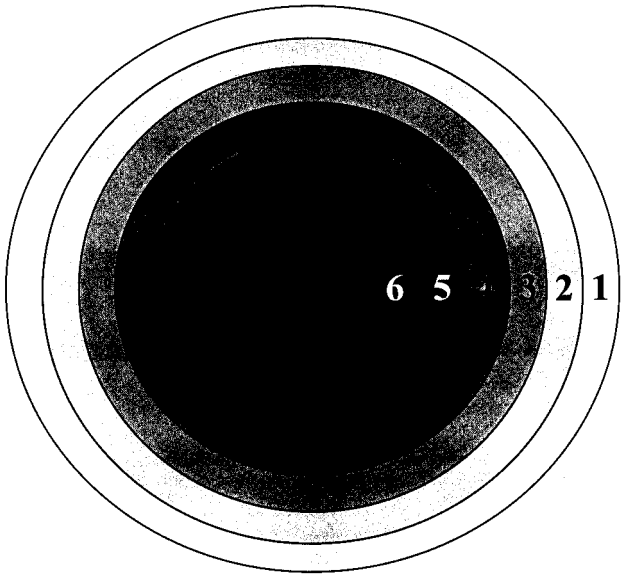

FIGURE 7 Partition of the protein into concentric shells. The outermost six shells (labeled 1–6) were fitted with the analytical dynamical model.

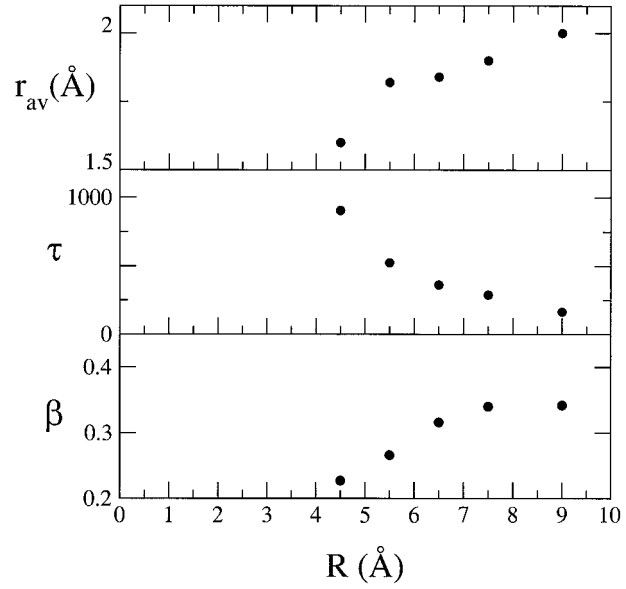

FIGURE 9 Smooth variation of dynamical parameters with distance, R, from the center of mass of the protein.

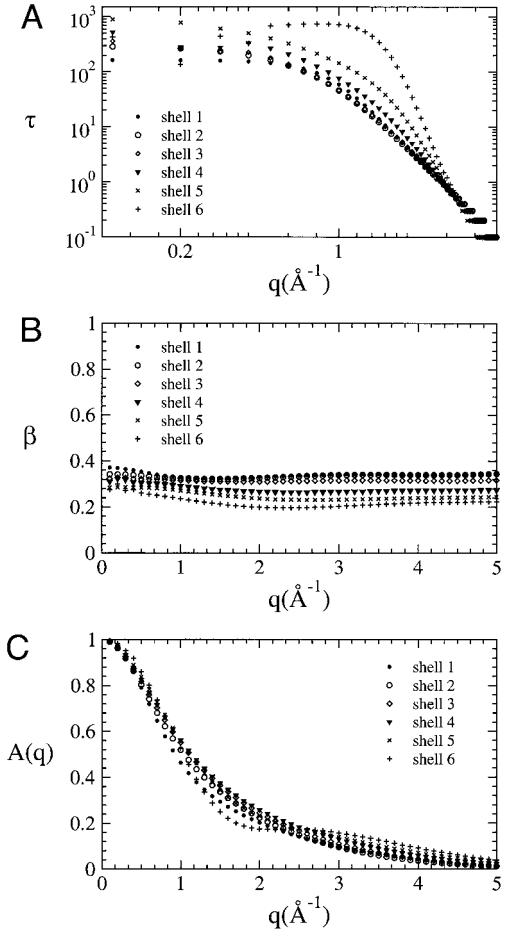

FIGURE 8 Shell dependence of the dynamical parameters. (A) τ versus q. (B) β versus q. (C) $A(q)$ versus q.

illustrated in Fig. 7. The shells were 1-Å thick with the exception of the inner- and the outer-most, which were 2-Å thick to include a reasonable number of atoms.

It was found that the analytical model (Eq. 4) could be adequately fitted only for the six outermost shells of the protein (numbers 1–6 in Fig. 7). The reason for this is that the diffusive dynamics of the atoms of the innermost two shells are too slow to be probed with the present MD simulation and neutron instrument (i.e., they are >1 ns). However, because the six outermost shells contain ~95% of the protein atoms, a large fraction of the protein dynamics is covered in the present analysis.

The dependence of $A(q)$, $\tau(q)$ and $\beta(q)$, on q for the six fitted shells is presented in Fig. 8, *A–C*. For the innermost of the six shells (shell number 6), the $A(q)$ and $\tau(q)$ profiles differ from the rest and are consistent with the dominance of slower and more confined processes. For the outermost five shells $A(q)$, $\tau(q)$, and $\beta(q)$ vary monotonically with distance. Figure 9 presents the dependence of the three parameters on the distance from the protein core. The average radius of confined diffusion decreases gradually from 2 Å in the outermost shell to 1.6 Å in the fifth, in good agreement with the mean-square displacement averaged over the atoms of each shell (Fig. 10). Accompanying this effect, the stretch factor β reduces by ~40%, from 0.35 to 0.20, indicating that moving toward the center increases the range of timescales spanned by the dynamical relaxation processes. Finally, τ increases from 160 to 800 ps, smoothly shifting toward slower relaxations when moving toward the center of the protein.

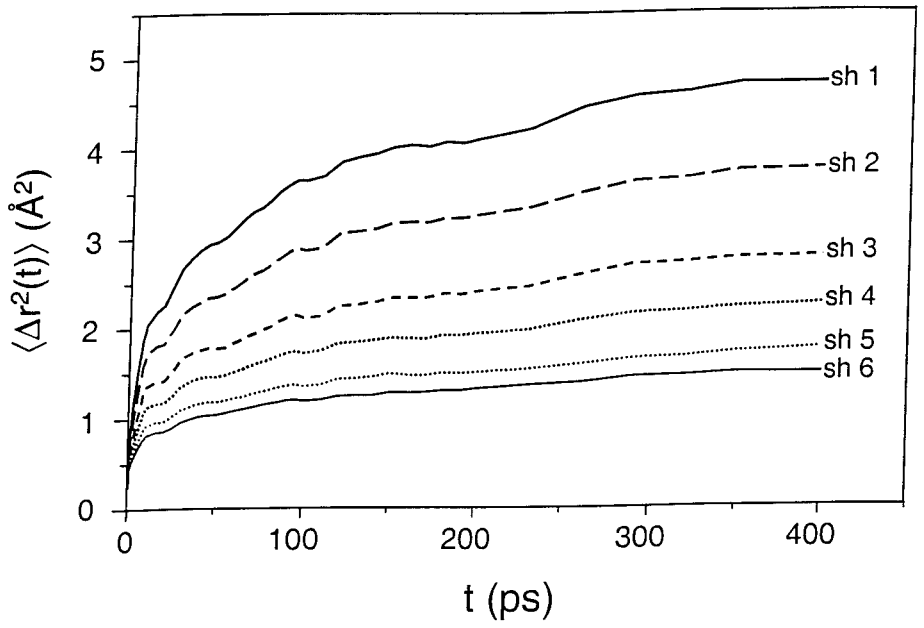

FIGURE 10 Shell-dependence of the mean-square displacement.

CONCLUSION

The present model, derived by combining quasielastic neutron scattering, MD simulation, and analytical modeling, captures in a simple way the range of amplitudes and timescales of the internal diffusive motions in different parts of a protein. The relationships between experiment, simulation, and the obtention of a simplified dynamical description should be clearly understood. The simplified dynamical model cannot be extracted directly from the neutron scattering experiment because the experiment is not discriminating enough. In other words, the present neutron-scattering results alone cannot be used to derive the "radial softening" description (although this might in the future be possible experimentally with some specific deuterium labeling). Here, the experimental data are used as a check that the amplitudes and timescales of the diffusive motions in the simulation are approximately correct, and the simulation is then analyzed to determine the simplified dynamical model.

The agreement between experiment and simulation is not perfect. This is expected, partly because the simulation is not fitted to the experiment because the MD method does not contain independent parameters that can be meaningfully adjusted for this purpose. However, the comparison here and in previous work (Dellerue et al., 2000; Kneller and Smith, 1994; Smith, 1991; Smith et al., 1990; Cusack et al., 1988) indicates that basic features of protein quasielastic scattering are reproduced by the MD.

Analysis of the simulation-derived intermediate scattering function reveals clear stretched exponential behavior, placing proteins on common ground with many strongly-interacting disordered systems such as glass-forming liquids. Analysis of the q-dependence of the parameters obtained provides further information on the nature of the motions involved. As presented in Fig. 4, the q-dependence of τ in a protein is typical for confined diffusion. Although the diffusion-in-a-sphere model is only a crude representation of the detailed motions present in the protein, the present results show that it captures the essence of the displacements contributing to the quasielastic neutron scattering. An alternative would be to model the atoms as jumping between rotamer positions. However, it was shown in Kneller and Smith (1994) that the motion principally contributing to quasielastic scattering from proteins at 300 K is not rotamer transition but rather is continuous diffusion. This finding was confirmed in a later study (Steinbach and Brooks, 1996).

The dynamics of a protein depends on its environment (Ansari et al., 1987; Reat et al., 2000). Determination of the environmental dependence of the dynamical parameters investigated in the present work would therefore be of much interest. The experiment and simulation were performed at a hydration level (0.52 g/g) at which the dynamics of a protein as seen by neutrons is essentially that of a fully-hydrated protein.

The physical picture of a globular protein arising from the present analysis is as follows. First, specific differences are seen between the backbone and side-chain dynamics. The average sphere radius for the backbone atoms is significantly smaller than for the side chains and the time dependence less nonexponential, indicating a narrower spread of distribution of relaxation times. The

marked difference between the backbone and side-chain dynamics suggests a physical similarity of a protein to composite materials formed from a "hard" (backbone) and a "soft" (side chains) component. Second, and perhaps most important, new light is shed on the dynamics as a function of the distance from the center of the protein. Previous simulation and experimental work on hydrated proteins has revealed significant differences between the dynamics of the surface and the interior residues (e.g.,. Zhou et al., 1999; Perez et al., 1999; Loh et al., 1999; Stella et al., 1999; Sopkova et al., 1999; Feng et al., 1998). The present results are consistent with this, but further reveal a monotonic variation of dynamical parameters with distance from the protein core. Both the amplitudes of confined diffusion and the relaxation parameters change smoothly from the surface to the interior (Fig. 9). The ~40% decrease of the stretch factor β as one goes deeper into the protein is consistent with spreading of the relaxation times over larger and larger intervals. Accompanying this τ gradually increases fivefold, from 160 to 800 ps, indicating a shift toward slower relaxation processes. Some of the very slowest processes, concerning particularly the 3-Å central core of the protein, remain unsampled both by the 1-ns simulation and by the neutron instrument used.

The smooth decrease of mobility moving toward the interior of the protein can be correlated with recent crystallographic data on human α-lactalbumin that indicate a radial variation of the magnitude of isotropic temperature factors (Harata et al., 1999). It is also consistent with, and might provide an explanation for, the observation that, during denaturation, a protein becomes less structured radiating away from the core (Daggett et al. 1996). The model of dynamics emerging from the present data can readily be represented by a shell model describing the gradual change in dynamical parameters. This "radially-softening" model of depth-dependent protein dynamics is consistent with a picture in which internal reorganization of protein atoms becomes progressively more difficult as one approaches the core. This may provide a protein with the local flexibility required for ligand binding while preserving the stability of its tertiary structure. Furthermore, the present results suggest that the protein glass transition might be also radially-dependent. This means that, as the temperature decreases, the diffusive dynamics on any given time scale would first freeze out in the center of a protein, then progressively freeze out with increasing distance from the center. This possibility could, in principle, be investigated experimentally, using neutron scattering with specific hydrogenation of residues at selected distances from the center of mass in an otherwise perdeuterated protein.

REFERENCES

Ansari, A., J. Berendzen, D. Braunstein, B. R. Cowen, H. Frauenfelder, M. K. Hong, I. E. Iben, J. B. Johnson, P. Ormos, T. B. Sauke, et al. 1987. Rebinding and relaxation in the myoglobin pocket. *Biophys. Chem.* 26:337–355.

Amadei, A., B. L. de Groot, M. A. Ceruso, M. Paci, A. Di Nola, and H. J. Berendsen. 1999. A kinetic model for the internal motions of proteins: diffusion between multiple harmonic wells. *Proteins.* 35:283–292.

Arbe, A., J. Colmenero, M. Monkenbusch, and D. Richter. 1998. Dynamics of glass-forming polymers: 'homogenous' versus 'heterogenous' scenarios. *Phys. Rev. Lett.* 81:590–593.

Balabin, I. A., and J. N. Onuchic. 2000. Dynamically controlled protein tunneling paths in photosynthetic reaction centers. *Science.* 290: 114–117.

Bee, M. 1988. Quasielastic Neutron Scattering. Principles and Application in Solid State, Chemistry, Biology and Material Science. Adam Higler, Bristol and Philadelphia, PA.

Bellissent-Funel, M.-C., J. Teixeira, K. F. Bradley, and S. H. Chen. 1992. Dynamics of hydration water in proteins. *J. Phys. I (France).* 2:995–1001.

Bellissent-Funel, M. C., A. Filabozzi, and S. H. Chen. 1997. Measurement of coherent Debye–Waller factor in in vivo deuterated C-phycocyanin by inelastic neutron scattering. *Biophys. J.* 72:1792–1799.

Blumen, A., and H. Schnorer. 1990. Fractals and related hierarchical models in polymer science. *Angew. Chem. Int. Ed. Engl.* 29:113–125.

Brooks, B. R., R. E. Bruccoleri, B. D. Olafson, D. J. States, S. Swaminathan, and M. Karplus. 1983. CHARMM: a program for macromolecular minimization and dynamics. *J. Comp. Chem.* 4:187–217.

Brooks, C. L. III, M. Karplus, and B. M. Petitt. 1988. Proteins: A Theoretical Perspective of Dynamics, Structure and Thermodynamics. John Wiley and Sons, New York.

Bu, Z., D. A. Neumann, S. H. Lee, C. M. Brown, D. M. Engelman, and C. C. Han. 2000. A view of dynamics changes in the molten globule-native folding step by quasielastic neutron scattering. *J. Mol. Biol.* 301:525–536.

Chen, S.-H., P. Gallo, and M.-C. Bellissent-Funel. 1995. Slow dynamics of interfacial water. *Can. J. Phys.* 73:703–709.

Cordone, L., M. Ferrand, E. Vitrano, and G. Zaccai. 1999. Harmonic behavior of trehalose-coated carbon-monoxy-myoglobin at high temperature. *Biophys. J.* 76:1043–1047.

Cusack, S., J. Smith, J. Finney, B. Tidor, and M. Karplus. 1988. Inelastic neutron scattering analysis of picosecond internal protein dynamics. Comparison of harmonic theory with experiment. *J. Mol. Biol.* 202: 903–910.

Daggett, V., A. Li, L. S. Itzhaki, D. E. Otzen, and A. R. Fersht. 1996. Structure of the transition state for folding of a protein derived from experiment and simulation. *J. Mol. Biol.* 257:430–440.

Daniel, R. M., J. L. Finney, V. Reat, R. Dunn, M. Ferrand, and J. C. Smith. 1999. Enzyme dynamics and activity: time-scale dependence of dynamical transitions in glutamate dehydrogenase solution. *Biophys. J.* 77: 2184–2190.

Daniel, R. M., J. C. Smith, M. Ferrand, S. Hery, R. Dunn, and J. L. Finney. 1998. Enzyme activity below the dynamical transition at 220 K. *Biophys. J.* 75:2504–2507.

Daragan, V. A., and K. H. Mayo. 1993. Tri- and diglycine backbone rotational dynamics investigated by ^{13}C NMR multipletrelaxation and molecular dynamics simulations. *Biochemistry.* 32:11488–11499.

Dellerue, S., A.-J. Petrescu, J. C. Smith, S. Longeville, and M.-C. Bellissent-Funel. 2000. Collective dynamics of a photosynthetic protein probed by neutron spin-echo spectroscopy and molecular dynamics simulation. *Physica B.* 276–278:514–515.

Diehl, M., W. Doster, W. Petry, and H. Schober. 1997. Water-coupled low-frequency modes of myoglobin and lysozyme observed by inelastic neutron scattering. *Biophys. J.* 73:2726–2732.

Dunn, R. V., V. Reat, J. Finney, M. Ferrand, J. C. Smith, and R. M. Daniel. 2000. Enzyme activity and dynamics: xylanase activity in the absence of fast anharmonic dynamics. *Biochem. J.* 346:355–358.

Elber, R., and M. Karplus. 1987. Multiple conformational states of proteins: a molecular dynamics analysis of myoglobin. *Science.* 235: 318–321.

Feng, W., R. Tejero, D. E. Zimmerman, M. Inouye, and G. T. Montelione. 1998. Solution NMR structure and backbone dynamics of the major cold-shock protein (CspA) from *Escherichia coli*: evidence for conformational dynamics in the single-stranded RNA-binding site. *Biochemistry.* 37:10881–10896.

Ferrand, M., A. J. Dianoux, W. Petry, and G. Zaccai. 1993. Thermal motions and function of bacteriorhodopsin in purple membranes: effects of temperature and hydration studied by neutron scattering. *Proc. Natl. Acad. Sci. U.S.A.* 90:9668–9672.

Fitter, J., O. P. Ernst, T. Hauss, R. E. Lechner, K. P. Hofmann, and N. A. Dencher. 1998. Molecular motions and hydration of purple membranes and disk membranes studied by neutron scattering. *Eur. Biophys. J.* 27:638–645.

Frauenfelder, H., S. Sligar, and P. Wolynes. 1991. The energy landscapes and motions of proteins. *Science.* 254:1598–1603.

Frauenfelder, H., P. J. Steinbach, and R. D. Young. 1988. Conformational substates in proteins. *Annu. Rev. Biophys. Biophys. Chem.* 17:451–479.

Goldstein, R. A., Z. A. Luthey-Schulten, and P. G. Wolynes. 1992. Protein tertiary structure recognition using optimized Hamiltonians with local interactions. *Proc. Natl. Acad. Sci. U.S.A.* 89:9029–9033.

Götze, W., and L. Sjögren. 1992. Relaxation processes in supercooled liquids. *Rep. Prog. Phys.* 55:241–376.

Harata, K., Y. Abe, and M. Muraki. 1999. Crystallographic evaluation of internal motion of human alpha-lactalbumin refined by full-matrix least-squares method. *J. Mol. Biol.* 287:347–358.

Hayward, S., A. Kitao, and N. Go. 1995. Harmonicity and anharmonicity in protein dynamics: a normal mode analysis and principal component analysis. *Proteins.* 23:177–186.

Heikal, A. A., S. T. Hess, G. S. Baird, R. Y. Tsien, and W. W. Webb. 2000. Molecular spectroscopy and dynamics of intrinsically fluorescent proteins: coral red (dsRed) and yellow. *Proc. Natl. Acad. Sci. U.S.A.* 97:11996–12001.

Hinsen, K., A.-J. Petrescu, S. Dellerue, M.-C. Bellissent-Funel, and G. Kneller. 2000. Harmonicity in slow protein dynamics. *Chem. Phys.* 261:25–37.

Jorgensen, W. L., J. Chandrasekhar, J. D. Madura, R. W. Impey, and M. L. Klein. 1983. Comparison of simple potential functions for simulating liquid water. *J. Chem. Phys.* 79:926–935.

Kneller, G. R., and J. C. Smith. 1994. Liquid like side-chain dynamics in myoglobin. *J. Mol. Biol.* 242:181–185.

Kurzinsky, M. 1998. A synthetic picture of intramolecular dynamics of proteins. Towards a contemporary statistical theory of biochemical processes. *Prog. Biophys. Mol. Biol.* 69:23–82.

Loh, A. P., W. Guo, L. K. Nicholson, and R. E. Oswald. 1999. Backbone dynamics of inactive, active, and effector-bound Cdc42Hs from measurements of (15)N relaxation parameters at multiple field strengths. *Biochemistry.* 38:12547–12557.

Ma, J., P. B. Sigler, Z. Xu, and M. Karplus. 2000. A dynamic model for the allosteric mechanism of GroEL. *J. Mol. Biol.* 302:303–313.

MacKerell. A. D., D. Bashford, M. Bellott, R. L. Dunbrak, J. D. Evanseck, M. J. Field, S. Fischer, J. Gao, H. Guo, S. Ha, D. Joseph-McCarthy, L. Kuchnir, K. Kuczera, F. T. K. Lau, C. Mattos, S. Michnick, T. Ngo, D. T. Nguyen, B. Prodhom, I. W. E. Reiher, B. Roux, M. Schlenkrich, J. C. Smith, R. Stote, J. Straub, M. Watanabe, J. Wiorkiewicz-Kuczera, D. Yin, and M. Karplus. 1998. All-atom empirical potential for molecular modeling and dynamics studies of proteins *J. Phys. Chem. B.* 102: 3586–3616.

McCammon, A. J., and S. C. Harvey. 1987. Dynamics of Proteins and Nucleic Acids. Cambridge University Press, Cambridge, UK.

Parak, F., E. N. Frolov, A. A. Kononenko, R. L. Mossbauer, V. I. Goldanskii, and A. B. Rubin. 1980. Evidence for a correlation between the photoinduced electron transfer and dynamic properties of the chromatophore membranes from *Rhodospirillum rubrum*. *FEBS Lett.* 17: 368–372.

Perez, J., J. M. Zanotti, and D. Durand. 1999. Evolution of the internal dynamics of two globular proteins from dry powder tosolution. *Biophys. J.* 77:454–469.

Rasmussen, B. F., A. M. Stock, D. Ringe, and G. A. Petsko. 1992. Crystalline ribonuclease A loses function below the dynamical transition at 220 K. *Nature.* 357:423–424.

Reat, V., R. Dunn, M. Ferrand, J. L. Finney, R. M. Daniel, and J. C. Smith. 2000. Solvent dependence of dynamic transitions in protein solutions. *Proc. Natl. Acad. Sci. U.S.A.* 97:9961–9966.

Reat, V., H. Patzelt, M. Ferrand, C. Pfister, D. Oesterhelt, and G. Zaccai. 1998. Dynamics of different functional parts of bacteriorhodopsin: H-2H labeling and neutron scattering. *Proc. Natl. Acad. Sci. U.S.A.* 95: 4970–4975.

Receveur, V., P. Calmettes, J. C. Smith, M. Desmadril, G. Coddens, and D. Durand. 1997. Dynamical change on denaturation of phosphoglycerate kinase revealed by quasielastic neutron scattering. *Proteins.* 28: 380–387.

Rykaert, J. P., G. Ciccotti, and H. J. C. Berendsen. 1977. Numerical integration of the Cartesian equations of motion of a system with constraints: molecular dynamics of *n*-alkanes. *J. Comput. Phys.* 23: 327–338.

Schlesinger, M. F. 1988. Fractal time in condensed matter. *Annu. Rev. Phys. Chem.* 39:269–290.

Sciortino, F., P. Gallo, P. Tartaglia, and S.-H. Chen. 1996. Supercooled water and the kinetic glass transition. II Collective dynamics. *Phys. Rev.* E54:6331–6343.

Sciortino, F., P. Gallo, P. Tartaglia, and S.-H. Chen. 1997. Molecular-Dynamics study of incoherent neutron scattering spectra of supercooled water. *Phys. Rev.* E56:4231–4223.

Smith, J. C., K. Kuczera, and M. Karplus. 1990. Temperature-dependence of myoglobin dynamics: neutron spectra calculated from molecular dynamics simulations of myoglobin. *Proc. Natl. Acad. Sci. U.S.A.* 87: 1601–1605.

Smith, J. C. 1991. Protein dynamics: comparison of simulations with inelastic neutron scattering experiments. *Quart. Rev. Biophys.* 24: 227–291.

Smith, J. C. 1997. Dynamics of biomolecules: simulations versus x-ray and neutron scattering experiments. *In* Computer Simulations of Biomolecules 3. Chap. 13. W. F. van Gunsteren, P. K. Weiner, and A. J. Wilkinson, editors. Kluwer/Escom, Leiden, The Netherlands. 305–360.

Smith, J. C. 2001. X-ray and neutron scattering as probes of biomolecular dynamics. *In* Computational Biochemistry and Biophysics. O. Becker, A. D. MacKerell, B. Roux, and M. Watanabe, editors. Marcel Dekker, New York. 237–251.

Sopkova, J., M. Vincent, M. Takahashi, A. Lewit-Bentley, and J. Gallay. 1999. Conformational flexibility of domain III of annexin V at membrane/water interfaces. *Biochemistry.* 38:5447–5458.

Souaille, M., F. Guillaume, and J. C. Smith. 1996a. Molecular dynamics analysis of alkane dynamics in urea inclusion compound. I. Comparison with quasielastic neutron scattering experiment. *J. Chem. Phys.* 105: 1516–1528.

Souaille, M., F. Guillaume, and J. C. Smith. 1996b. Molecular dynamics analysis of alkane dynamics in urea inclusion compound. II. Rotational distribution and elastic incoherent structure factor. *J. Chem. Phys.* 105: 1529–1536.

Stein, D. L. 1985. A model of protein conformational substates. *Proc. Natl. Acad. Sci. U.S.A.* 82:3670–3672.

Steinbach, P. J., and B. R. Brooks. 1996. Hydrated myoglobin's anharmonic fluctuations are not primarily due to dihedral transitions. *Proc. Natl. Acad. Sci. U.S.A.* 93:55–59.

Stella, L., M. Nicotra, G. Ricci, N. Rosato, and E. E. Di Iorio. 1999. Molecular dynamics simulations of human glutathione transferase P1–1: analysis of the induced-fit mechanism by GSH binding. *Proteins.* 37: 1–9.

Vitkup, D., D. Ringe, G. A. Petsko, and M. Karplus. 2000. Solvent mobility and the protein 'glass' transition. *Nat. Struct. Biol.* 7:34–38.

Volino, F., and A. Dianoux. 1980. Neutron incoherent scattering law for diffusion in a potential of spherical symmetry: general formalism and application to diffusion inside a sphere. *Mol. Phys.* 41:271–279.

Williams, G., and D. C. Watts. 1970. Non-symmetrical dielectric relaxation behavior arising from simple empirical decay function. *Trans. Faraday Soc.* 66:80–85.

Yamasaki, K., M. Saito, M. Oobatake, and S. Kanaya. 1995. Characterization of the internal motions of *Escherichia coli* ribonuclease HI by a combination of 15N-NMR relaxation analysis and molecular dynamics simulation:examination of dynamic models. *Biochemistry*. 34: 6587–6601.

Zaccai, G. 2000a. How soft is a protein? A protein dynamics force constant measured by neutron scattering. *Science.* 288:1604–1607.

Zaccai, G. 2000b. Moist and soft, dry and stiff: a review of neutron experiments on hydration-dynamics-activity relations in the purple membrane of *Halobacterium salinarum*. *Biophys. Chem.* 86:249–257.

Zanotti, J.-M., M. C. Bellissent-Funel, and J. Parello. 1997. Dynamics of a globular protein as studied by neutron scattering and solid-state NMR. *Physica B.* 234–236:228–230.

Zanotti, J.-M., M. C. Bellissent-Funel, and J. Parello. 1999. Hydration-coupled dynamics in proteins studied by neutron scattering and NMR: the case of the typical EF-hand calcium-binding parvalbumin. *Biophys. J.* 76:2390–2411.

Zhou, Y., D. Vitkup, and M. Karplus. 1999. Native proteins are surface-molten solids: application of the Lindemann criterion for the solid vs liquid state. *J. Mol. Biol.* 285:1371–1375. S